Korean J. Chem. Eng., 35(1), 44-52 (2018)
DOI: 10.1007/s11814-017-0248-1

pISSN: 0256-1115
eISSN: 1975-7220

Prediction of CO_2 mass transfer parameters to light oil in presence of surfactants and silica nanoparticles synthesized in cationic reverse micellar system

Mahshid Nategh*, Shahriar Osfouri*,†, and Reza Azin**

*Department of Chemical Engineering, Faculty of Petroleum, Gas, and Petrochemical Engineering, Persian Gulf University, Bushehr 7516913817, Iran
**Department of Petroleum Engineering, Faculty of Petroleum, Gas, and Petrochemical Engineering, Persian Gulf University, Bushehr 7516913817, Iran
(*Received 9 June 2017 • accepted 13 September 2017*)

Abstract−CO_2 miscible injection method combined with surfactants and silica nanoparticles was studied to investigate the effect of these additives on CO_2 mass transfer parameters to the light oil, including diffusion coefficient, mass transfer coefficient and solubility. Silica nanoparticles with controlled size distribution were synthesized in isooctane/1-hexanol/CTAB/ammonium hydroxide, a highly-stable reverse micellar system with w_o=5. The presence of Si-O-Si and Si-O-H bonds in FTIR spectra of the system revealed that silica nanoparticles are formed by partial hydrolysis of TEOS. Results of DLS indicated that the average size and size distribution of the synthesized nanoparticles were 27.6 nm and 13-76 nm, respectively. Diffusion tests were carried out using CO_2 gas and three liquid systems: isooctane/1-hexanol, isooctane/1-hexanol/CTAB reverse micellar system without nanoparticles, and isooctane/1-hexanol/CTAB reverse micellar system with nanoparticles. Results of modeling and optimization of the gas-liquid systems under non-equilibrium interface condition, using pressure decay data show that the presence of surfactants and nanoparticles leads to decreased gas diffusion coefficient; while increased interface mass transfer resistance due to presence of aqueous droplets and nanoparticles as well as lower solubility of CO_2 in the light oil are the results of applying these additives, which limits their application. The obtained CO_2 diffusion coefficients for isooctane/1-hexanol, reverse micellar system without nanoparticles, and reverse micellar system with nanoparticles are 8.5550×10^{-8}, 8.2216×10^{-8}, and 8.1114×10^{-8} m^2/s, respectively.

Keywords: Diffusion Coefficient, Mass Transfer Coefficient, Light Oil, CO_2 Injection, Surfactant, Silica Nanoparticles

INTRODUCTION

Due to the increasing demand for energy and the possibility of extracting only one-third of the in-situ oil from reservoirs using common production methods, utilizing enhanced oil recovery (EOR) methods for production of the remaining oil is of great importance [1-5]. Among EOR methods, CO_2 miscible injection has received great attention [6]. Considering that CO_2 is a greenhouse gas with increasing concentration in the atmosphere, it can be used for EOR purposes alongside reducing its environmental issues [7]. However, despite its great potential, this method has faced some problems and limitations during its application.

Recently, nanotechnology and, especially, nanoparticles [2,3] have been studied extensively with the goal of improving EOR methods with IFT reduction [8-10], wettability alteration [11-14], increasing the viscosity of injecting fluid [15], increasing the stability, durability, and efficiency of microemulsions [16-19]. However, the application of nanoparticles combined with miscible injection method needs to be further investigated. For example, size distribution of nanoparticles is a very important parameter in nano-based EOR methods, because the uncontrolled size distribution results in pore blockage and irreparable damage to the reservoir. Among the common methods for synthesis of nanoparticles, the reverse micelle system, composed of dispersed and continuous phase, has a great potential for synthesis of nanoparticles with controlled size distribution in order to overcome the blockage problem [20,21].

On the other hand, in spite of the fact that surfactants and nanoparticles combined with miscible injection method have been noticed in literature, their effectiveness and impact on major flow parameters, i.e., gas flow pattern and mass transfer parameters, have not been studied specifically. For a gas injection process, the effectiveness degree is mainly influenced by the gas dissolution rate into oil, which itself is controlled by molecular diffusion. Molecular diffusion leads to mixing of oil and injected gas, prevention of viscous fingering, postponing gas breakthorough and improving the sweep efficiency in a gas injection oil recovery process [22]. Thus, investigation of this mechanism in such processes is of great importance and many studies on this topic in hydrocarbon systems have been reported [23-28]. Considering that calculation of a diffusion coefficient is complicated without experimental measurements, two indirect and direct experimental methods are utilized for this purpose. In the direct method, the alteration of composition of diffusing component in liquid column with time is analyzed directly with an analytical device. However, this method is

†To whom correspondence should be addressed.
E-mail: osfouri@pgu.ac.ir, osfouri@hotmail.com

not well accepted due to low accuracy and disturbance imposed on system as a result of sampling. While, in the indirect method, one of the system properties such as gas concentration or pressure is recorded and the rate of its change is correlated with concentration change [23]. Computer assisted tomography (CAT), dynamic pendant drop shape analysis, NMR spectra change and pressure decay are some other methods, among which the latter is most accepted due to the desired level of simplicity and accuracy [29]. The first researcher who mathematically modeled the diffusion process in gas-liquid systems using pressure decay data in order to calculate diffusion coefficient and mass transfer coefficient was Riazi [25]. Since then, many other models have been developed. For example, Shaikha et al. [23] calculated the diffusion coefficient of of methane, carbon dioxide, and nitrogen in bitumen by graphical method and calculation of Henry's constant from gas solubility, using the assumptions of no liquid swelling due to gas diffusion, and constant gas compressibility factor. Zhang et al. investigated the diffusion coefficient in CO_2/heavy oil system by integrating the diffusion equations between the initial and final time and graphical method [24]. They assumed no swelling, constant compressibility factor, equal amount of CO_2 leaving the gas phase and entering the liquid phase. Civan and Rasmussen [28,30-32] introduced film mass transfer resistance parameter at the interface, defined as reciprocal of mass transfer coefficient, k, to the model and utilized a Robin-type boundary condition at the interface to estimate the values of diffusion coefficient and mass transfer coefficient. Etminan et al. proposed an improved version of boundary condition at the interface when film mass trassfer resistance exists [27]. They applied a time-dependent Robin-type boundary condition that covers the whole range of equilibrium and non-equilibrium behaviors.

The necessity of this study is that despite many advantages of surfactants and nanoparticles, their applicability in large scale and in combination with miscible gas injection method has not been considered. Thus, this important issue must be thoroughly investigated by calculation of key mass transfer parameters. Additionally, considering that the possibility of liquid swelling due to gas dissolution may be high in the light and medium oil systems, evaluation of simplified models is necessary in order to find out that neglecting this factor may lead to deviation from real situation or not.

According to the aforementioned statements, the main goal of this study is to investigate the applicability of nanoparticles combined with miscible injection method, by investigating the gas diffusion coefficient, interface mass transfer coefficient and solubility, through modeling and optimization of the process using pressure decay data. Meanwhile, the influence of surfactants as well as blend of surfactants and nanoparticles on the above characteristics are explored. For this purpose, silica nanoparticles with controlled size distribution were synthesized using reverse micellar system and the reverse micellar system with highest stability was chosen for carrying out gas diffusion tests.

MATERIALS AND METHODS

1. Materials

CTAB (97% purity) and ammonium hydroxide 32 wt% (density: 0.88 g/ml) were purchased from Merck™, and tetraethyl orthosilicate (TEOS) (98% purity) was purchased from ACROS ORGANICS. Other chemicals such as isooctane (99.5% purity), 1-hexanol (98% purity) and ethanol (99.5% purity) were purchased from domestic companies. CO_2 (99.99% purity) gas cylinder was purchased from domestic suppliers.

2. Synthesis of Nanoparticles

Silica nanoparticles were synthesized in isooctane/1-hexanol/CTAB/ammonium hydroxide cationic reverse micellar system. In this step, based on our previous works, 20 mM CTAB in 10 ml isooctane/1-hexanol (v/v: 4/1) organic solvent was used as the initial solution [33]. Then, a certain amount of ammonium hydroxide 8.94 wt% proportional to w_o=5, 7 and 9 was added to the prepared solution and was shaken to obtain a transparent solution. Then, a given amount of TEOS proportional to water/TEOS molar ratio of 10 was added to the solution. The reason for choosing this ratio is that Arriagada and Osseo-Assare studied the synthesis of silica nanoparticles in NP-5/cyclohexane reverse micellar system and concluded that in water/TEOS molar ratios lower than stochiometric ratio, the ethanol/water ratio increases and the system becomes unstable by replacement of aqueous phase with ethanol; while more stable samples are formed at higher ratios [34,35]. Finally, the prepared solution was kept at room temperature for 24 hours with continuous shaking. A schematic of silica nanoparticles synthesis process in the reverse micellar system is shown in Fig. 1. Also, the amounts of materials used in three w_o cases are given in Table 1.

3. Diffusion Tests

Diffusion tests were carried out using diffusion apparatus containing three cells: gas, liquid, and diffusion cell, as depicted in Fig. 1. Details of the experimental apparatus used for diffusion tests are described by Azin et al. [36]. CO_2, isooctane/1-hexanol, isooctane/1-hexanol/CTAB reverse micellar system without nanoparticles, and isooctane/1-hexanol/CTAB reverse micellar system with nanoparticles, were used as gas and liquid systems, respectively (see Fig. 1). Isooctane can be regarded as a representive of reservoir oil. To carry out diffusion tests, the liquid systems were prepared; the diffusion cell was filled with the liquid and put in the air bath of the diffusion apparatus to reach the desired temperature. CO_2 entered the gas cell and when the read pressure did not change, the exit valve of the supplying cylinder was closed. In this situation, the read pressure showed the gas cell pressure. After that, liquid was injected by injection pump and after reaching the desired pressure, the valve of gas cell was closed. In the final step, the change of pressure with time was recorded by the software. The specifications of diffusion tests in this study are tabulated in Table 2.

As the main objective of this study was to investigate the effect of surfactant and nanoparticles on miscible gas injection method, we just needed constant operating conditions, i.e., constant temperature and initial pressure for comparison purposes between three liquid systems.

MATHEMATICAL MODELING

In light oil systems, a constant diffusion coefficient and constant compressibility factor may not be applied due to concentration

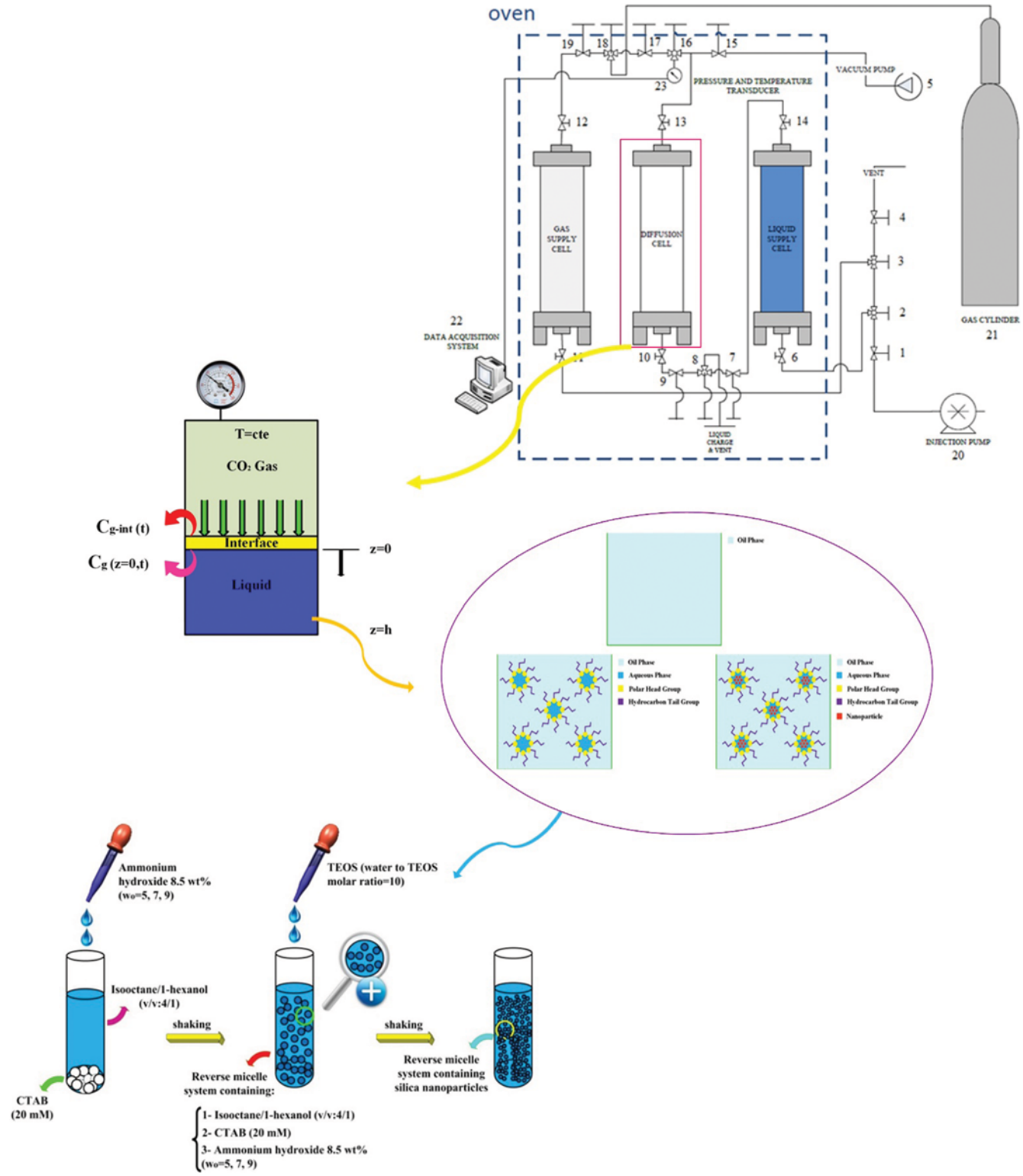

Fig. 1. A scheme of diffusion apparatus, diffusion cell with mass transfer resistance at interface, liquid systems, and silica nanoparticles synthesis process in the reverse micellar system.

dependency and high pressure change, respectively. Also, applying Henry's law due to higher solubility of CO_2 in light oil does not seem to result in high accuracy. Moreover, neglecting oil swelling as consequence of gas dissolution seems to be irrational. However, to investigate the significance of these assumptions and their impact on the final results, in this study, the Etminan model [27] with non-equilibrium condition at interface, i.e., in presence of mass transfer resistance at interface, was chosen for calculation of diffu-

Table 1. Materials used in synthesis of silica nanoparticles

w_o (mol/mol)	CTAB (mg)	NH_4OH (μl)	TEOS (μl)
5	72.80	22.46	22.16
7	72.80	31.45	31.03
9	72.80	40.43	39.89

sion coefficient, mass transfer coefficient and gas solubility. A schematic representation of diffusion cell is given in Fig. 1 and the main assumptions used in this study are as follow:

1. Temperature is kept constant throughout the test.
2. Diffusion is one-dimensional in the axial direction. This is true when the ratio of height of the cell to its diameter is higher than 2.5 [24]. In this study, the liquid height was 10 cm and its diameter was 3.81 cm (L/D=2.625).
3. There is no chemical reaction between CO_2 and liquid system.
4. The liquid system is unvolatile and unidirectional diffusion from gas to liquid phase is considered.
5. Diffusion coefficient is constant.
6. Compressibility factor is constant.

Based on the physics of the system and the above assumptions, the diffusion equation (Fick's second law) and boundary and initial conditions in Cartesian coordinate are written according to Eqs. (1)-(4).

$$\frac{\partial C_g}{\partial t} = D\frac{\partial^2 C_g}{\partial z^2} \tag{1}$$

$$\frac{\partial C_g(z=h,\, t)}{\partial z} = 0 \tag{2}$$

$$-D\frac{\partial C_g}{\partial z} = k[C_{g-int}(t) - C_g(z=0,\, t)] \tag{3}$$

$$C_g(z,\, t=0) = 0 \tag{4}$$

Applying Henry's law for gas concentration above the interface, Eq. (5) is derived.

$$C_{g-int}(t) = \frac{P(t)}{H} \tag{5}$$

Rewriting the boundary condition at interface, leads to Eq. (6).

$$\frac{\partial C_g}{\partial z} = M\frac{\partial C_g}{\partial t} - N\left[\frac{\partial^2 C_g}{\partial t \partial z}\right] \tag{6}$$

where M and N are defined as:

$$M = \frac{V_g M_w H}{ARTZD} \tag{7}$$

$$M = \frac{V_g M_w H}{ARTZk} \tag{8}$$

By correlating the rate of mass transfer from gas phase and rate of gas dissolution in liquid phase, the solution of diffusion equation is obtained in Laplace domain:

$$\overline{C}_g(z,\, s) = \frac{MP_i\left[\exp\left((z-2h)\sqrt{\frac{s}{D}}\right) + \exp\left(-z\sqrt{\frac{s}{D}}\right)\right]}{H\left[\left(Ms+(1+Ns)\sqrt{\frac{s}{D}}\right) + \exp\left(\left(-2h\sqrt{\frac{s}{D}}\right)\left(Ms-(1+Ns)\sqrt{\frac{s}{D}}\right)\right)\right]} \tag{9}$$

where $\overline{C}_g$ is the gas concentration in the Laplace domain and s denotes the variable of frequency domain. The analytical Laplace inverse of Eq. (9) is not available, and numerical techniques like Stehfest algorithm [37] is applied to obtain the inverse form numerically. By replacing $C_{g-int}(t)$ in Eq. (3) from Eq. (5), Eq. (10) is derived.

$$P(t) = -\frac{DH}{k}\frac{\partial C_g}{\partial z}\bigg|_{z=0} + HC_g(z=0,\, t) \tag{10}$$

Then, the calculated pressure in Laplace doamain is obtained as:

$$\overline{P}_{cal}(z,\, s) = -\frac{DH}{k}\frac{\partial \overline{C}_g}{\partial z}\bigg|_{z=0,\, s} + H\overline{C}_g(z=0,\, s) \tag{11}$$

Differentiating Eq. (9) and substituting in Eq. (11) gives Eq. (12):

$$\overline{P}_{cal}(z,\, s) = \frac{MP_i\left[\exp\left(-2h\sqrt{\frac{s}{D}}+1\right) - \frac{D}{k}\left(\sqrt{\frac{s}{D}}\exp\left(-2h\sqrt{\frac{s}{D}}\right) - \sqrt{\frac{s}{D}}\right)\right]}{\left[\left(Ms+(1+Ns)\sqrt{\frac{s}{D}}\right) + \exp\left(-2h\sqrt{\frac{s}{D}}\right)\left(Ms-(1+Ns)\sqrt{\frac{s}{D}}\right)\right]} \tag{12}$$

The calculated pressure is obtained using the above equation and an inverse Laplace transform algorithm. In this study, Gaver-

Table 2. The specifications of diffusion tests in this study

Initial pressure (MPa)	5.672±0.01
Temperature (K)	311.15
Liquid phase	Isooctane/1-hexanol Isooctane/1-hexanol/CTAB reverse micellar system without nanoparticles Isooctane/1-hexanol/CTAB reverse micellar system with nanoparticles
Gas phase	CO_2
Initial CO_2 concentration in liquid phase (kg/m^3)	0
Liquid height (m)	0.10
Gas cap height (m)	0.25
Cell cross sectional area (m^2)	0.001139
Gas cap volume (m^3)	0.00028475
Liquid volume (m^3)	0.0001139

Stehfest algorithm [37] was used for this purpose and a mathematical model was coded for simulation of diffusion process using a homemade modeling environment in MATLAB software. Then, the calculated pressure by Etminan model [27] was compared with the experimental pressure from pressure decay tests by defining an objective function as Eq. (13):

$$SE=\sum_{i=1}^{N}[P_{exp}(t)-P_{cal}(t)]^2 \quad (13)$$

Differential evolution (DE) technique, which is a simple, powerful population based, stochastic function minimizer, was applied for optimization purpose and a DE MATLAB code was used for obtaining the values of diffusion coefficient (D), mass transfer coefficient (k) and Henry's constant (H).

RESULTS AND DISCUSSION

1. Mechanism of Synthesis of Nanoparticles

To ensure the synthesis and investigate the mechanism of silica nanoparticles formation, FTIR spectroscopy was carried out on synthesized particles in the reverse micellar phase. FTIR-460 plus Jasco instrument was used to record the spectra in the range of 400-4,000 cm^{-1} with an effective resolution 4 cm^{-1} at room temperature. In addition, the average size and size distribution of synthesized nanoparticles were determined using dynamic light scattering (DLS) particle size analyzer HORIBA LB-550. For each sample, 50 acquisitions were averaged. To increase accuracy of measurement and eliminate temperature effects on the size, the temperature of the cell holder was adjusted at room conditions.

To track the reactions in the reverse micelles, FTIR spectra of three reverse micellar samples are illustrated in Fig. 2. The first sample was prepared in the absence of TEOS. The second and third ones containing TEOS were taken 1 and 24 hours after preparation, respectively. In the absence of TEOS, only C-H peaks are observed in 2,849.31 cm^{-1} which can be attributed to CTAB organic groups. On the other hand, the presence of TEOS results in the appearance of Si-O-Si, Si-O and OH peaks in 1,056.8, 919.879 and 3,336.25 cm^{-1}. These peaks confirm the formation of silica nanoparticles in the reverse micelle system through reactions given in Table 3.

Table 3. Reactions in silica nanoparticles synthesis process

Reactions	
$Si(OC_2H_5)_4+xH_2O\rightarrow -Si(OC_2H_5)_{4-x}(OH)x+xC_2H_5OH$	(1)
$Si-OC_2H_5+Si-OH\rightarrow -Si-O-Si-+C_2H_5OH$	(2)
$Si-OH+Si-OH\rightarrow -Si-O-Si-+H_2O$	(3)

Comparing the absorbance of these peaks suggests that the reaction goes to completion after 24 hours and the concentration of the produced silica nanoparticles increases. Formation of incomplete silica lattice and presence of Si-O bonds can be explained by the fact that in the alkaline environment, the surface of hydrolyzed species (i.e., Si-OH) is deprotonated and becomes negatively charged. Therefore, there are a few silanol neutral species available in the aqueous phase. These neutral species are condensed after hydrolysis reaction and form Si-O-Si bonds. However, due to the repulsion between homonymous charges, the negatively charged species cannot condense and complete the silica lattice.

2. Nanoparticles' Size and System Stability

DLS results for silica particles synthesized in the reverse micellar system with w_o=5, 7 and 9 are revealed in Fig. 3(a), 3(b) and 3(c), respectively.

In w_o=5, the average size and size distribution of the silica nanoparticles was 27.6 and 13-76 nm, respectively. However, for systems with w_o=7 and 9, the silica particles were micro-sized, and gel was formed after 24 hours. Formation of ethanol (reactions 1 and 2) might be one of the reasons for gel formation [34,35]. Also, CTAB reaction with OH^- and SiO^- can lead to decomposition of

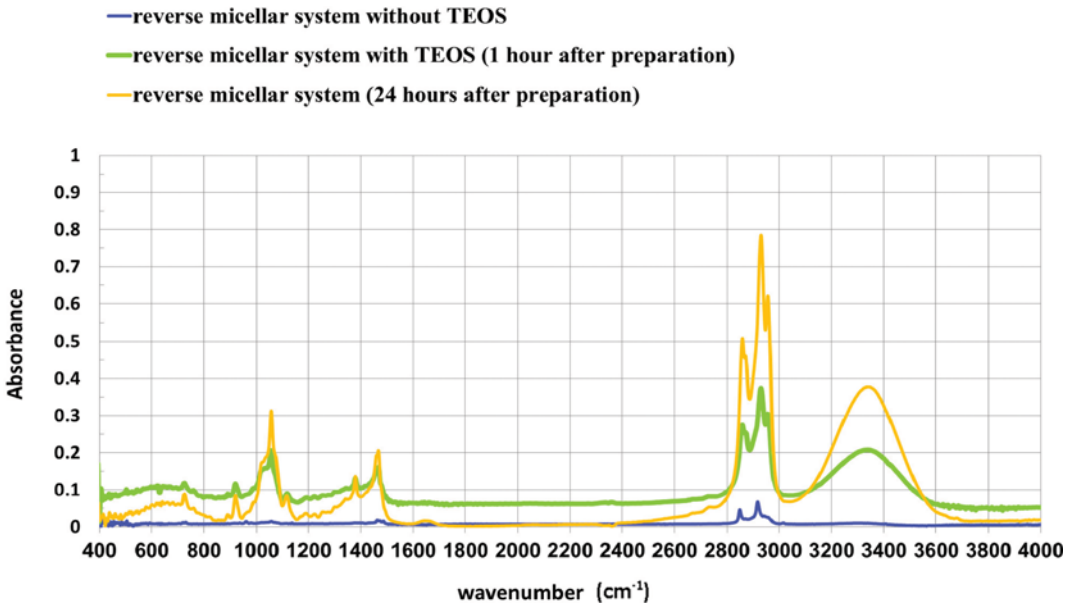

Fig. 2. FTIR spectra of reverse micellar systems.

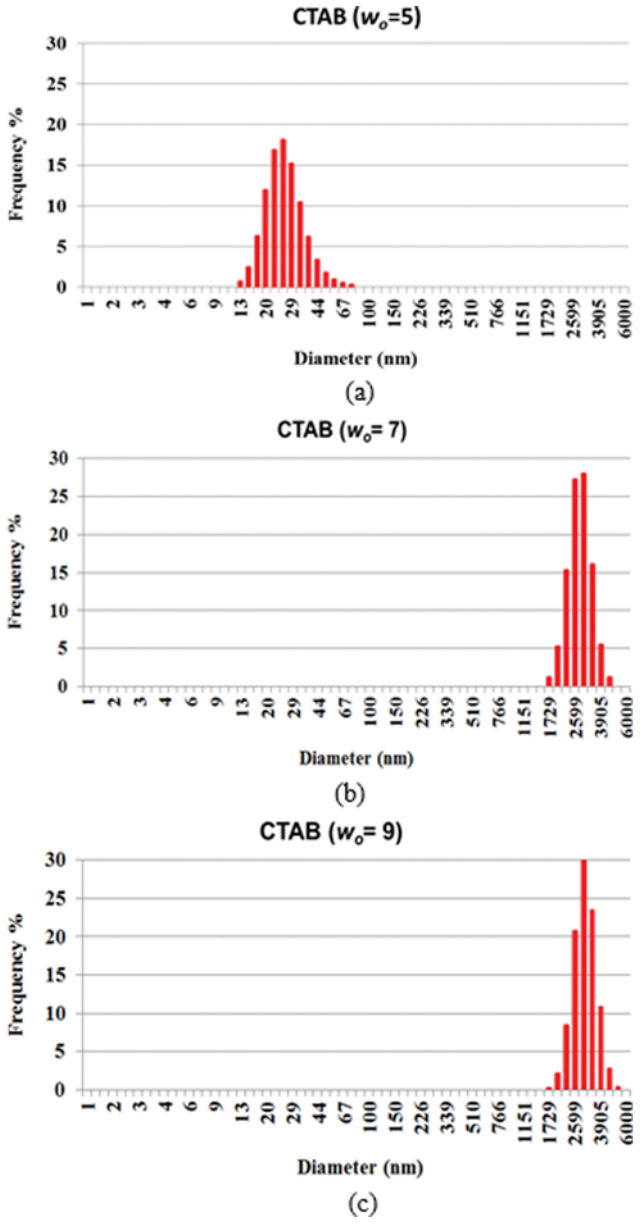

Fig. 3. DLS results of silica nanoparticles in the reverse micellar system. (a) w_o=5, (b) w_o=7, (c) w_o=9.

the surfactant layer and consequently destroying reverse micelles [38]. On the other hand, consuming some of the deprotonated species leads to pH reduction, which in turn results in the reduction of negative charge of silica solution. Therefore, more species remain neutral which can form gel in the separated aqueous bulk phase [39].

It was observed that the reverse micellar system remains stable after 24 hours for the system with w_o=5. This may be the due to presence of ethanol by-product in the organic phase rather than in aqueous phase. Hence, phase separation caused by replacement of aqueous phase with ethanol, followed by agglomeration of nanoparticles does not occur [35]. Also, the solution is less alkaline with lower pH at this w_o, and fewer hydrolyzed species become deprotonated. As a result, less OH^- and SiO^- species react with CTAB; this in turn prevents decomposition of reverse micellar system. Since system stability and size distribution of nanoparticles are two main parameters in EOR methods, a reverse micellar system with w_o=5 with and without nanoparticles was selected for diffusion tests.

Exact timing was scheduled to carry out the DLS tests in a very stable condition and no CTAB degradation for three systems containing silica nanoparticles. Therefore, the difference in the size distribution of three systems is just due to difference in nanoparticles' sizes and not to the surfactant degradation. The degradation of the system occurred in a longer time.

3. Gas Diffusion in Liquids

CO_2 diffusion coefficient in water has been investigated thoroughly by our team in previous studies [40,41]. In this study, CO_2 mass transfer parameters to light oil were evaluated. Considering the Etminan model used in this study, the calculated pressure was obtained using the Gaver-Stehfest inverse Laplace transform algorithm and optimization used the DE algorithm. For this purpose, a program was coded for simulation of the diffusion process using a homemade modeling environment in MATLAB software. The initial pressure for all of the tests was 5.672 MPa, which is below the critical pressure of CO_2 to avoid reaching the supercritical phase of CO_2 that may cause error.

The experimental data obtained from tests for three oil systems are listed in Table 4.

The pressure decay data and calculated pressure from Etminan model after optimization for three oil systems are plotted in Figs. 4, 5 and 6. Also, the optimized parameters obtained for three systems under study are tabulated in Table 5. These figures and table obviously reveal that ignoring swelling factor in the systems under study has not led to a significant error in prediction of pressure. Fig. 7 compares the optimized values of H, k, and D for three systems under study.

As can be observed from Table 4, the amount of pressure decay and equilibrium time for isooctane/1-hexanol system is higher and lower, respectively, than the other two systems. This has led to higher gas diffusion coefficient for this system (see Table 5). The order of data involving diffusion coefficient, mass transfer coefficient and Henry's constant reported in Table 5 is in agreement with the data for CO_2-light oil system in the literature [29]. Additionally, the dif-

Table 4. Experimental data obtained for three liquid systems

Liquid system	Initial pressure (MPa)	Equilibrium pressure (MPa)	Equilibrium time (hours)
Isooctane/1-hexanol	5.672±0.01	4.0662	38
Isooctane/1-hexanol/CTAB reverse micellar system without nanoparticles	5.672±0.01	4.1293	40
Isooctane/1-hexanol/CTAB reverse micellar system with nanoparticles	5.672±0.01	4.1605	43

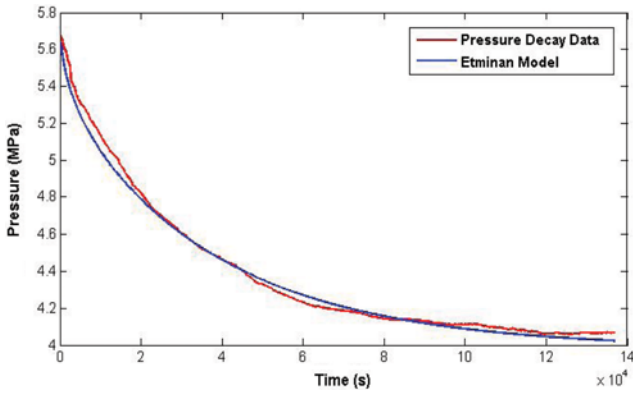

Fig. 4. Experimental pressure decay data and calculated pressure from Etminan model for isooctane/1-hexanol.

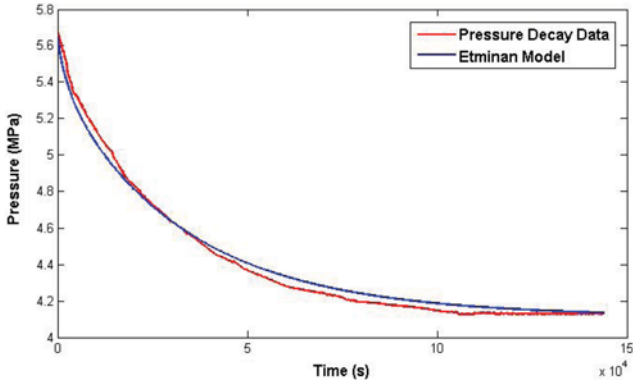

Fig. 5. Experimental pressure decay data and calculated pressure from Etminan model for reverse micellar system without nanoparticles.

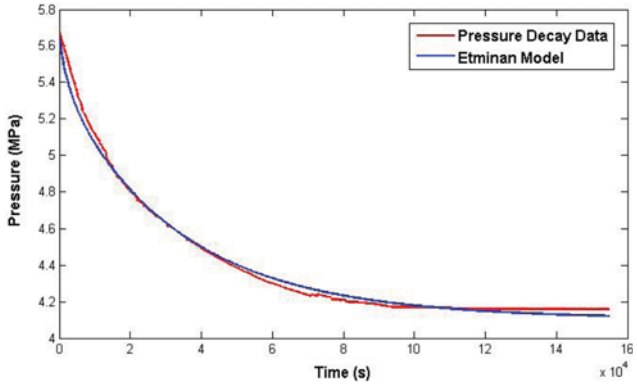

Fig. 6. Experimental pressure decay data and calculated pressure from Etminan model for reverse micellar system with nanoparticles.

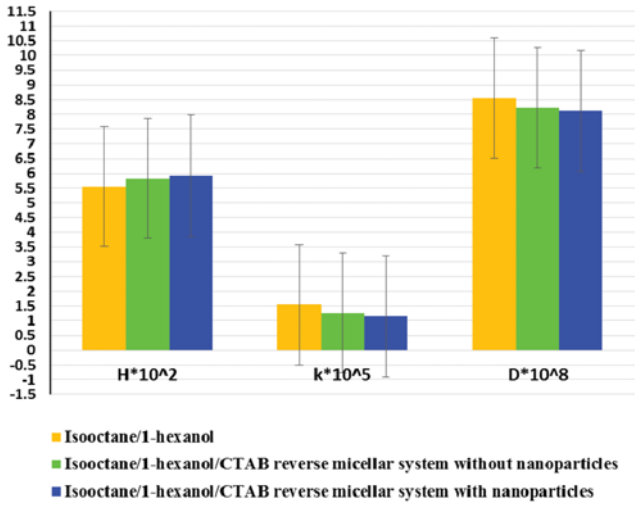

Fig. 7. Comparison of mass transfer parameters obtained from optimization for CO_2 diffusion in three liquid systems.

fusion coefficient for reverse micellar system without nanoparticles is lower than isooctane/1-hexanol system and higher than reverse micellar system with silica nanoparticles. These results confirm that the higher the diffusion coefficient, the shorter it takes for the interface concentration to reach the equilibrium. Also, Henry's constant is higher for reverse micellar system with silica nanoparticles, which reveals lower equilibrium concentration at interface as well as lower gas solubility in liquid. This, in turn, results in shorter pressure decay. These results are in agreement with Etminan et al. [27].

On the other hand, the interface mass transfer coefficient for three liquid systems follows the following order:

Reverse micellar system with nanoparticles<Reverse micellar system without nanoparticles<Isooctane/1-hexanol system

This occurs due to the presence of particles or reverse micelle droplets in the liquid phase, which leads to increasing the resistance to mass transfer at interface and lowering the mass transfer coefficient. The reason for this is the lower solubility of CO_2 in dispersed aqueous phase than in continuous oil phase, which is clear by comparing the results of Henry's constants obtained in this study for continuous hydrocarbon phase and those obtained for aqueous systems by Drummond [42]. Various researchers have also confirmed that the presence of particles and droplets can enhance the rate of gas-liquid mass transfer only when the solubility of the gas solute in the dispersed phase is higher than in the continuous liquid phase [43-47].

Fig. 7 reveals that the increment or reduction in the results is higher in first and second liquid systems, while it diminishes in

Table 5. Optimized parameters obtained for three systems under study

Liquid system	Henry constant ($MPa \cdot m^3/kg$)	Mass transfer coefficient (m/s)	Diffusion coefficient (m^2/s)	Error
Isooctane/1-hexanol	5.5436×10^{-2}	1.5350×10^{-5}	8.5550×10^{-8}	6.4719×10^{-2}
Isooctane/1-hexanol/CTAB reverse micellar system without nanoparticles	5.8322×10^{-2}	1.3645×10^{-5}	8.2216×10^{-8}	6.6623×10^{-2}
Isooctane/1-hexanol/CTAB reverse micellar system with nanoparticles	5.9212×10^{-2}	1.2422×10^{-5}	8.1114×10^{-8}	6.5822×10^{-2}

the second and third systems. On the other hand, altering the liquid to reverse micellar system, which includes surfactants and aqueous dispersed phase, leads to higher change in the obtained results; however, adding nanoparticles to the reverse micellar system results in reduced amount of changes. This indicates that effect of surfactants and aqueous droplets is higher on the mass transfer behavior; however, the presence of nanoparticles also has its effect.

In this study, oil swelling due to gas dissolution was not taken into account and the results revealed that ignoring the swelling seems reasonable. However, to predict the swelling behavior of these three systems and the effect of surfactants and nanoparticles on liquid swelling, the interactions between molecules present in these systems should be considered. Since isooctane occupies the highest percent of liquid volume in three liquid systems, three major types of interactions of isooctane/isooctane, isooctane/CO_2, and CO_2/CO_2 should be noted. Higher swelling is expected for the system with higher solubility of CO_2 in oil system. The reason is that under these circumstances, isooctane/CO_2 interaction is more favorable and results in higher swelling [48]. This should be further investigated in detail by implying molecular simulations.

CONCLUSION

CTAB reverse micellar system was utilized as an effective method for controlled size distribution of silica nanoparticles in order to avoid blockage of reservoir rock pores. Comparison of the FTIR spectra taken from CTAB reverse micellar systems at different times confirms that synthesis of silica nanoparticles in the reverse micelle nanoreactors is carried out during hydrolysis and condensation reactions. Results showed that the system is stable for w_o=5, and silica nanoparticles are formed with average size and size distribution of 27.6 nm and 13-76 nm, respectively. Investigating the effect of surfactants and silica nanoparticles with controlled size on CO_2 miscible injection for three liquid systems revealed that the diffusion coefficient, mass transfer coefficient (inverse of mass transfer resistance at interface) and gas solubility are lower for systems containing nanoparticles and surfactants. This is a determining result which limits the application of these additives in combination with miscible injection method. Comparing the modeling results with experimental data indicated that that Etminan model with non-equilibrium boundary condition at interface, which has been proposed for heavy oils, describes the CO_2 diffusion behavior well for the three light oil systems under study. Due to the specific properties of nanoparticles, more tests should be carried out in the presence of nanoparticles in porous media to investigate their effect on gas diffusion; this is proposed because gas diffusion mechanism and rate is different in porous media due to different forces and fluid flow behavior.

NOMENCLATURE

A : diffusion cell cross sectional area [m^2]
C : mass concentration [kg/m^3]
D : diffusion coefficient [m^2/s]
H : Henry's law constant [$MPa \cdot m^3/kg$]
h : height of liquid column [m]
k : film mass transfer coefficient [m/s]
M : group of coefficients
M_w : molecular weight [kg/kgmole]
N : group of coefficients
n : water/TEOS ratio
P : pressure [MPa]
R : universal gas constant, 0.0083144 [$MPa \cdot m^3/kg \cdot mol \cdot K$]
s : variable of frequency domain
T : absolute temperature [K]
t : time [s]
V : volume [m^3]
w_o : water/surfactant ratio
Z : gas compressibility factor
z : vertical spatial coordinate [m]

Subscripts

cal : calculated
exp : experimental
eq : equilibrium
g : gas
i : initial condition
int : interface

Abbreviations

DLS : dynamic light scattering
TEOS : tetraethyl orthosilicate
CTAB : cetyltrimethylammonium bromide
FTIR : fourier transform infrared
NP-5 : nonylphenol ethoxylate-5
SE : squared error

REFERENCES

1. X. kong and M. M. Ohadi, *Applications of micro and nano technologies in the oil and gas industry: An overview of the recent progress* Abu-Dhabi International Petroleum Exhibition and Conference, Abu-Dhabi, UAE (2010).
2. S. Kapusta, L. Balzano and P. Riele, *Nanotechnology applications in oil and gas exploration and production*, International Petloleum Technology Conference, Bangkok, Thailand (2012).
3. A. J. P. Fletcher and J. P. Davis, *How EOR can be transformed by nanotechnology*, The SPE Improved Oil Recovery Symposium, Tulsa, Oklahoma, U.S.A. (2010).
4. R. Sen, *Prog. Energy Combust. Sci.*, **34**, 714 (2008).
5. G. J. Hirasaki, C. A. Miller and M. Puerto, *SPE J.*, **16**, 889 (2011).
6. S. Kokal and A. Al-Kaabi, *Enhanced Oil Recovery: Challenges & Opportunities*, World Petroleum Council: Official Publication, 64 (2010).
7. J. G. J. Olivier, G. Janssens-Maenhout, M. Muntean and J. A. H. W. Peters, *Trends in global CO_2 emissions: 2013 Report*, PBL Netherlands Environmental Assessment Agency, Netherlands (2013).
8. A. Roustaei, J. Moghadasi, H. Bagherzadeh and A. Shahrabadi, *An experimental investigation of polysilicon nanoparticles' recovery efficiencies through changes in interfacial tension and wettability alteration*, SPE International Oilfield Nanotechnology Conference, Noordwijk, The Netherlands (2012).

9. L. Hendraningrat, L. Shidong, O. Torsater and S. Torsater, *A glass micromodel experimental study of hydrophilic nanoparticles retention for EOR project*, SPE Russian Oil and Gas Exploration and Production Technical Conference and Exhibition, Moscow, Russia (2012).
10. N. Y. T. Le, D. K. Pham, K. H. Le and P. T. Nguyen, *Adv. Nat. Sci.: Nanosci. Nanotechnol.*, **2**(3), 035013 (2011).
11. A. Maghzi, S. Mohammadi, M. H. Ghazanfari, R. Kharrat and M. Masihi, *Exp. Therm Fluid Sci.*, **40**, 168 (2012).
12. A. Maghzi, A. Mohebbi, R. Kharrat and M. H. Ghazanfari, *Transp. Porous Media.*, **87**, 653 (2011).
13. A. Karimi, Z. Fakhroueian, A. Bahramian, N. Pour Khiabani, J. Babaee Darabad, R. Azin and S. Arya, *Energy Fuels*, **26**(2), 1028 (2012).
14. B. Ju, T. Fan and Z. Li, *J. Pet. Sci. Eng.*, **86-87**, 206 (2012).
15. R. D. Shah, Application of nanoparticle saturated injectant gases for EOR of heavy oil, SPE annual technical conference and exhibition (2009).
16. T. Zhang, A. Davidson, S. L. Bryant and C. Huh, Nanoparticle-stabilized emulsions for applications in enhanced oil recovery, SPE Improved Oil Recovery Symposium, Tulsa, Oklahoma, U.S.A. (2010).
17. F. Qiu and D. Mamora, Experimental study of solvent-based emulsion injection to enhance oil recovery in Alaska North Slope area, Canadian Unconventional Resources & International Petroleum Conference, Calgary, Alberta, Canada (2010).
18. F. Qiu, The potential applications in heavy oil EOR with the nanoparticle and surfactant stabilized solvent-based emulsion, Canadian Unconventional Resources and International Petroleum Conference, Calgary, Alberta, Canada (2010).
19. V. Malhotra, Effects of mixed stabilizers (nanoparticles and surfactant) on phase inversion and stability of emulsions, Thesis, University of Waterloo (2009).
20. J. N. Solanki and Z. V. P. Murthy, *Ind. Eng. Chem. Res.*, **50**(22), 12311 (2011).
21. J. Eastoe, M. J. Hollamby and L. Hudson, *Adv. Colloid Interface Sci.*, **128-130**, 5 (2006).
22. P. Guo, Z. Wang, P. Shen and J. Du, *Ind. Eng. Chem. Res.*, **48**(19), 9023 (2009).
23. H. Sheikha, M. Pooladi-Darvish and A. K. Mehrotra, *Energy Fuels*, **19**(5), 2041 (2005).
24. Y. P. Zhang, C. L. Hyndman and B. B. Maini, *J. Pet. Sci. Eng.*, **25**(1-2), 37 (2000).
25. M. R. Riazi, *J. Pet. Sci. Eng.*, **14**(3-4), 235 (1996).
26. C. Yang and Y. Gu, *Ind. Eng. Chem. Res.*, **44**(12), 4474 (2005).
27. R. Etminan, M. Pooladi-Darvish, B. B. Maini and Z. Chen, *Fuel*, **105**, 672 (2013).
28. M. L. Rasmussen and F. Civan, *AIChE J.*, **55**, 1 (2009).
29. O. V. Trevisan, S. V. Araujo, R. G. D. Santos and J. A. Vargas, Diffusion coefficient of CO_2 in light oil under reservoir conditions using X-Ray Computed Tomography, Offshore Technology Conference (2013).
30. F. Civan and M. L. Rasmussen, *SPE J.*, **6**(2), 171 (2001).
31. F. Civan and M. L. Rasmussen, *Improved Measurement of Gas Diffusivity for Miscible Gas Flooding Under Nonequilibrium vs. Equilibrium Conditions*, SPE/DOE Improved Oil Recovery Symposium, Tulsa, Oklahoma (2002).
32. F. Civan and M. L. Rasmussen, *SPE J*, **11**(1), 71 (2006).
33. A. Haghtalab and S. Osfouri, *Sep. Sci. Technol.*, **38**(3), 553 (2003).
34. L. Yao, G. Xu, W. Dou and Y. Bai, *Colloids Surf., A Physicochem. Eng. Asp.*, **316**, 8 (2008).
35. F. J. Arriagada and K. Osseo-Asare, *Colloids Surface*, **69**, 105 (1992).
36. R. Azin, M. Mahmoudy, S. M. Jafari Raad and S. Osfouri, *Central European J. Eng.*, **3**, 585 (2013).
37. H. Stehfest, *Communication of the ACM*, **13**(1), 47 (1970).
38. D. Lv, W. Wen, X. Huang, J. Bai, J. Mi, S. Wu and Y. Yang, *J. Mater. Chem.*, **21**, 9506 (2011).
39. F. J. Arriagada and K. Osseo-Asare, *J. Colloid Interface Sci.*, **170**, 8 (1995).
40. Y. Gholami, R. Azin, R. Fatehi, S. Osfouri and A. Bahadori, *J. Mol. Liq.*, **201**, 23 (2015).
41. Y. Gholami, R. Azin, R. Fatehi and S. Osfouri, *J. Mol. Liq.*, **202**, 31 (2015).
42. S. E. Drummond, Boiling and mixing of hydrothermal fluids: chemical effects on mineral precipitation, PhD Thesis, Pennsylvania State University (1981).
43. V. Linek and P. Beneš, *Chem. Eng. Sci.*, **31**(11), 1037 (1976).
44. B. H. Junker, T. A. Hatton and D. I. Wang, *Biotechnol. Bioeng.*, **35**(6), 578 (1990).
45. F. Yoshida, T. Yamane and Y. Miyamoto, *Ind. Eng. Chem. Process Des. Dev.*, **9**(4), 570 (1970).
46. J. D. McMillan and D. I. C. Wang, *Ann. N. Y. Acad. Sci.*, **506**(1), 569 (1987).
47. A. Mimura, T. Kawano and R. Kodaira, *J. Ferment. Technol.*, **47**, 229 (1969).
48. J. Zhang, Z. Pan, K. Liu and N. Burke, *Energy Fuels*, **27**(5), 2741 (2013).